389. Fellenius, B.H., Massarsch K.R., Terceros M.H., and Terceros, M.A., 2018. A study of the augmenting effect of equipping piles with an Expander Body. Proc. of DFI-EFFC International Conference on Deep Foundations and Ground Improvement, Rome , June 6 - 8, 2018., pp. 114-123.

A STUDY OF THE AUGMENTING EFFECT OF EQUIPPING PILES WITH AN EXPANDER BODY

Bengt H. Fellenius[1)], K. Rainer Massarsch[2)], Mario Terceros H.[3)], and Mario Terceros A.[4)]

[1)]Consulting Engineer, 2475 Sidney, BC, Canada, V8L 2B9. <Bengt@fellnius.net>
[2)]Geo Risk & Vibration Scandinavia AB, Bromma, Sweden. <rainer.massarsch@georisk.se>
[3)]Incotec S.A., Santa Cruz de la Sierra, Bolivia <math@incotec.cc>
[4)]Incotec S.A., Santa Cruz de la Sierra, Bolivia <mta@incotec.cc>

ABSTRACT. A full-scale study is reported of the response of four pairs of piles of 150 mm through 620 mm diameter, bored piles drilled with slurry, continuing-flight auger-cast pile (CFA), and a full-displacement pile (FDP). One of each pair was equipped with an Expander Body to increase the pile-toe diameter, preload the pile axially, as well as bring about a stiffer pile toe and, thus, achieve a stiffer pile. All piles were constructed to 9.5 m depth in a loose to dense silty to dense sand. The EB-equipped piles were supplied with bidirectional cell immediately above the EB (depth 8.3 m). Static loading tests performed on all piles showed that the expansion of the EB markedly increased the pile toe stiffness. This, not just by increasing the pile toe area, but also by preloading the soil underneath the pile toe and increasing the shaft resistance acting around the 1.5 m long EB.

Keywords. Bored piles, CFA piles, Full Displacement piles, static loading test, pile-toe augment.

INTRODUCTION

The pile testing programme at the ISSMGE TC212 research site in Santa Cruz, the Bolivian Experimental Site for Testing Piles (B.E.S.T.) was organized in conjunction with the 3rd International Conference on Deep Foundations, April 27 – 29, 2017, in Santa Cruz de la Sierra, Bolivia. The programme included static loading tests on piles with and without a toe augment, an expandable device (Expander Body, EB), to increase the pile toe area and to improve the pile toe resistance. Four types of piles were constructed in pairs to 9.5 m depth in a silty to dense sand**:**

(Piles A) 620-mm diameter pile drilled with slurry
(Piles B) 450-mm diameter continuous flight auger pile
(Piles C) 450-mm diameter full displacement pile
(Piles D) 150 mm diameter gravity-grouted micro-pile

Each pair had one pile with an EB and one without. A head-down static loading test was carried out on the piles without an EB. The four EB-piles, were tested using a bidirectional test. The purpose of the here reported tests was to compare the static response of piles with and without an EB.

SOIL PROFILE

The site investigation at the B.E.S.T. site, the soil exploration, notably the CPTU sounding results, showed the soil profile to consist of essentially two soil layers: an upper 6 m thick layer of loose silt and sand on compact silty sand. The CPTU pore pressure measurements indicated a groundwater table at or near about 0.5-m depth and a hydrostatically distributed pore pressure. Figure 1 shows a diagram compiling the SPT N-indices and the CPTU cone stress, q_t. All in-situ test results at B.E.S.T., including pressuremeter and dilatometer tests, are available at the conference web site. The link to the site is: http://www.cfpbolivia.com/web/page.aspx?refid=157.

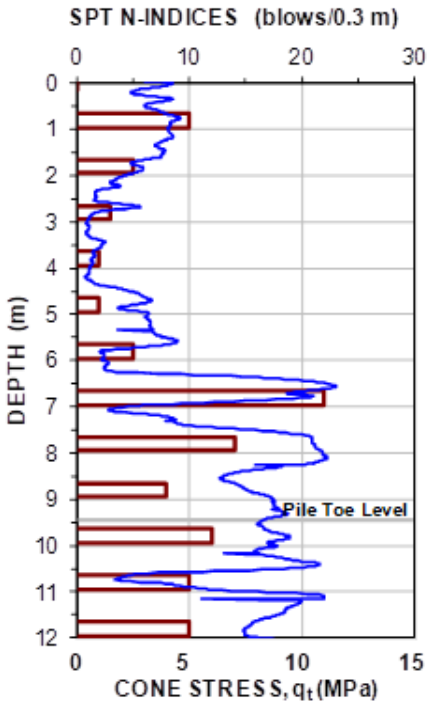

Fig. 1. SPT N-indices compiled with the CPTU q_t-stress at Pile A3.

THE EXPANDER BODY (EB)

The EB is a 1 to 2 m long folded, 120 mm wide steel tube that is expanded (inflated) by a primary-phase pressure-grouting delivered through a grouting tube placed in the reinforcing cage (Figure 2). Different models allow for expansion to 400 through 800 mm diameter width. Pressure and volume of the grout during the expansion of the EB are continuously recorded. The lateral expansion of the EB causes the length of the EB tube to shorten by about 100 mm, manifested as a lifting of the EB bottom-end or, in loose or soft soil, a pull-down of the shaft. As the EB is connected to the pile reinforcing cage, the expansion imposes tension in the pile and, potentially, a soil decompression below the expanded EB. The latter is offset by a second-phase grouting of the soil at the pile toe. The second-phase grout is delivered to the toe through a separate grout tube inside the grout tube (passing through the EB). Maximum grouting pressure below the EB is typically of the same magnitude as the EB-expansion pressure. For the here presented test piles, it was about 1.0 through 2.5 MPa. To compare, in-air tests have shown that about 100 kPa pressure is needed to expand the unconfined EB.

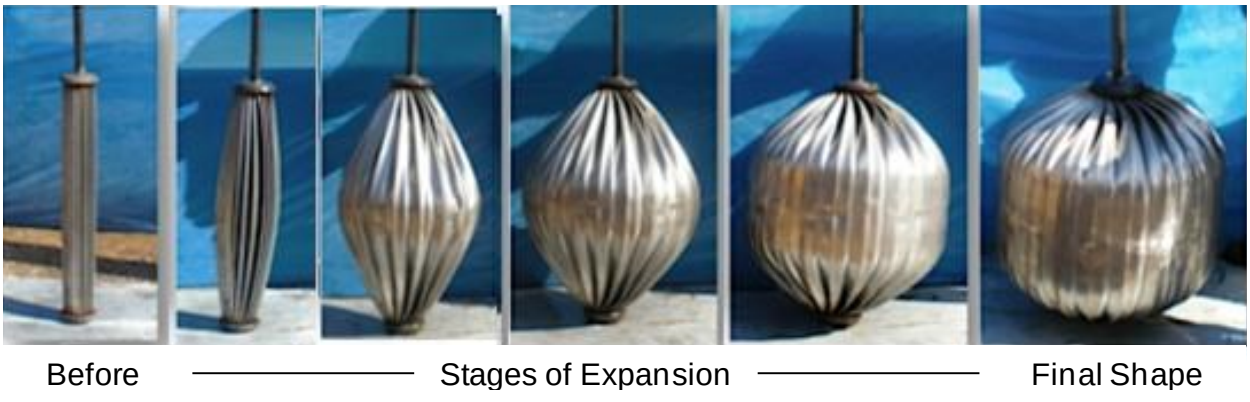

Fig. 2. In-air demonstration of EB expansion.

Figure 3 shows a sketch of the pile and EB arrangement at the B.E.S.T. site. The EB original length was 1.20 m and a bidirectional cell (hydraulic jack) jack, 300 mm high by 220 mm wide, was connected to the top of the EB and reinforcing cage.

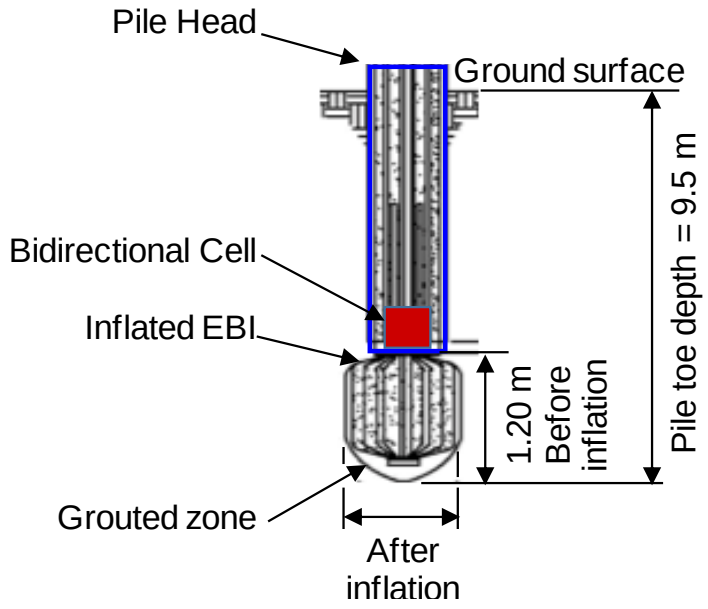

Fig. 3. Sketch showing the EB and BD arrangement (not to scale).

TEST PILES

The details of the test piles are listed in Table 1.

Table 1. Pile description.

Type		BD EB	Final EB Volume (L)	Final Pressure (MPa)	Estimated EB and TB width (mm)	Shaft Grouting Method
150-mm micro pile	D1	EB	130	1.1	400	Gravity
150-mm micro pile	D2	- - -				Gravity
450 mm CFA pile	B1	BD+EB	200	1.0	500	Pressure
450 mm CFA pile	B2	- - -				Pressure
620 mm Bored Pile	A1	BD+EB	245	2.3	600	Gravity
620 mm Bored Pile	A3	- - -				Gravity
450 mm FDP pile	C1	BD+EB	210	2.0	500	Pressure
450 mm FDP pile	C2	- - -				Pressure

BD = bidirectional jack, EB = Expander Body with post-grouting below EB (maximum pressure: 2.5 MPa).

TEST RESULTS

The static loading tests, bidirectional (BD) and head-down (HD) tests, were carried out by applying equal increments of load holding the load level constant for ten minutes. Tests on piles with BD jack and EB device started with the BD test followed by the HD test. In each static loading test—bidirectional as well as head-down—the applied load and movement along with readings of strain at three strain-gage levels (2.0, 5.0 and 7.5 m depth) were recorded.

Bored piles, Piles A and D, comparison of head-down test results

Piles A1 and A3 and D1 and D2 and were bored with slurry and gravity-grouted. Piles A1 and A3 were 620-mm diameter with a nominally 0.3019 m^2 cross section area and Piles D1 and D2 were micro piles with a nominally 0.0177 m^2 cross section area. Piles A1 and D1 were equipped with an EB at 8.3 m depth, while Piles A3 and D2 had no such augment. Strain values between the construction of the piles and start of the test were not recorded. Pile A1 was tested using a bidirectional cell placed immediately above the EB at 8.3 m depth. In Pile D2, the strains recorded during the tests were small and erratic. In contrast, the strain records in Pile A3 were consistent. Due to small strains and to the residual force in the pile (induced when the EB expanded), the strain records in Piles A1 and D1 are of limited value.

Figure 4A shows the Pile A3 (620-mm pile without an EB) pile-head load-movement curve. After assessing the load-movement curve, a "target point" (835 kN load at 30 mm movement), on the curve was chosen and the target load was matched in an effective stress analysis using proportionality coefficients (ß) for the shaft and a unit toe resistance for the toe movement (target pile-head movement minus pile compression). For the 0 to 6.0 m soil layer consisting of loose silt and sand ß = 0.40 was used. For the 6.0 to 9.5 m layer consisting of compact silty sand, ß = 0.60 was used. (N.B., the shear resistance does not occur as slippage, but as shear within a band of soil of small, but unknown, thickness). A unit pile toe stress, r_t, equal to 1.0 MPa, was used in the fit to the target point (at a 29-mm pile toe target movement). The analysis, using the UniPile software (Goudreault and Fellenius 2014), then continued by trying out different t-z and q-z functions, assuming and adjusting the function coefficients for the shaft and toe resistances until obtaining a simulated load-movement curve that fitted the measured curve. The adjustments were for the shape of the t-z and q-z curves, the resistance values that gave the fit to the at target point were not changed. (Background and mathematics of the t-z/q-z functions are presented in Fellenius 2016). The so-simulated pile-head, pile-toe, and pile-compression curves are shown along with the measured Pile A3 load-movement curve.

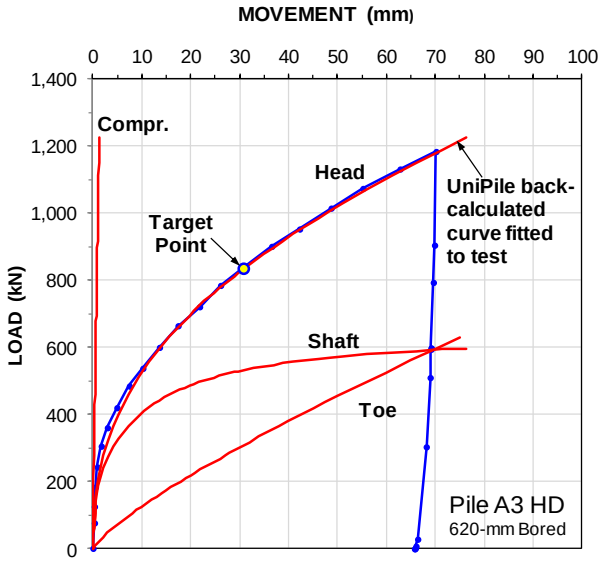

Fig. 4A Pile A3 load-movement curves.

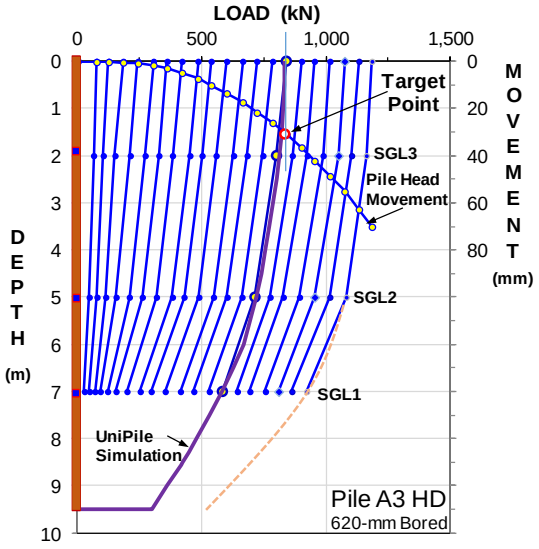

Fig. 4B Pile A3 load distribution.

Figure 5A shows the pile-head load-movement curve and the load distribution of the test on Pile D2 (150-mm micro-pile without an EB) and Figure 5B shows the simulated load distribution for the target load (144 kN at 15 mm movement) and includes also the distribution determined from the strain-gage values. The strain-gage values were too small and erratic for meaningful evaluation. The load-distribution graph is supplemented with the CPTU q_t-distribution and the load-movement curve with the target point indicated.

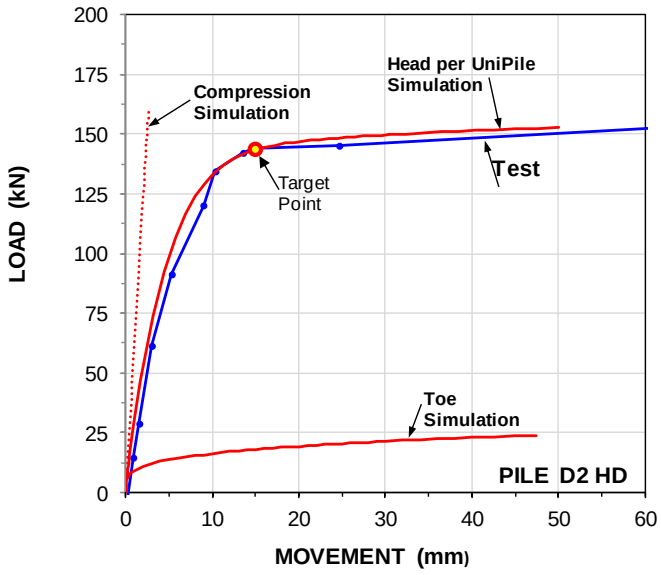

Fig. 4A. Pile D2 load-movement curves.

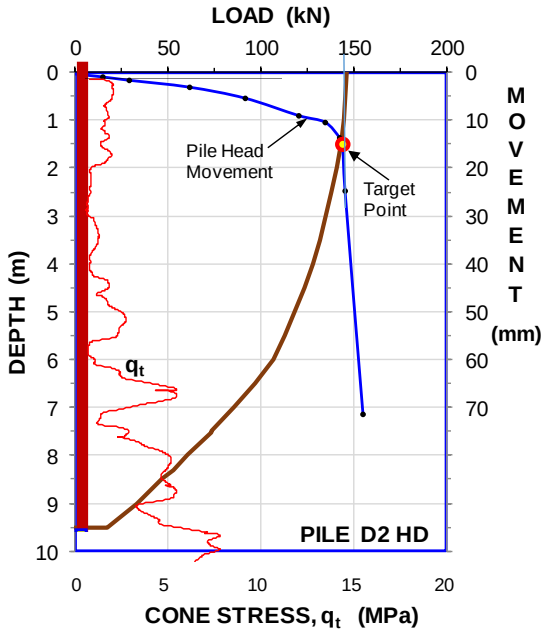

Fig. 4B. Pile D2 load distribution.

The target point for Pile D2 was chosen because it was produced with the same beta-coefficients and the same target toe stress as used for the analysis of Pile A3. However, the movement necessary for the coincidence to the target load of the beta-coefficients and the pile toe unit stress, was precisely twice for the analysis of the Pile A3 records as for the Pile D2 records. Pile A3 has a four times larger diameter and a 16 times larger toe area. The movement difference is indicated in comparing Figures 4A and 5A and in Figures 6 and 7 for the Pile A3 and D2 shaft resistance t-z functions and Figure 8 for the toe resistance q-z functions, respectively, used to obtain the load-movement fit for Piles D2 and A3. The "δ" indicates the movement for the target point and the "100 %" indicates the target resistance for the soil-pile elements. The t-z and q-z functions are quite different and the fact that the ß-coefficients and unit toe resistance values are the same is essentially a coincidence. Comparing the t-z and q-z curves shows that Piles A3 and D2 actually responded very differently to the applied load.

Figure 9A shows the simulated bidirectional-test load-movement curve of Pile A1 (identical to Pile A3, but for the EB at the pile toe). Figure 9B shows the Pile A1 simulated load distribution for the target load and includes also the calculated equivalent head-down load distribution. (the same Beta-coefficients were used above the BD, which gave 682 kN load at 5 mm upward and 1.7 mm downward movements). The strain-gage at 2.0 m depth did not function and the strain recorded by the gages at 5.0 m and 7.5 m depth were too small (<40 με) to allow conversion to load. However, the bidirectional test provides the benefit that the load applied and measured by the bidirectional device (hydraulic jack) is the true load. That is, it includes any potential residual force, unlike strain-gage instrumentation, which always requires consideration of adjustment to potential residual force in the pile. Thus, the "Target Point bidirectional load" is a true load.

Similarly, Figure 10A shows the simulated test curves head-down load-movement curve of Pile D1 (identical to Pile D2, but for the EB at the toe of Pile D1). Figure 10B shows the Pile D1 load-distributions. Again, the same beta-coefficients were used, which gave a 550 kN target point at 7 mm movement. The test records, notably, the strain-gage records, indicated that residual force had developed in the pile before the static loading test, but they were not consistent enough to warrant analysis. The dashed set of pile-head and toe load-movement curves in the figure are a speculative set of load-movement curves for the test had it been unaffected by residual force. (The procedure and decisions for establishing the distribution unaffected by residual force is beyond the scope of this paper).

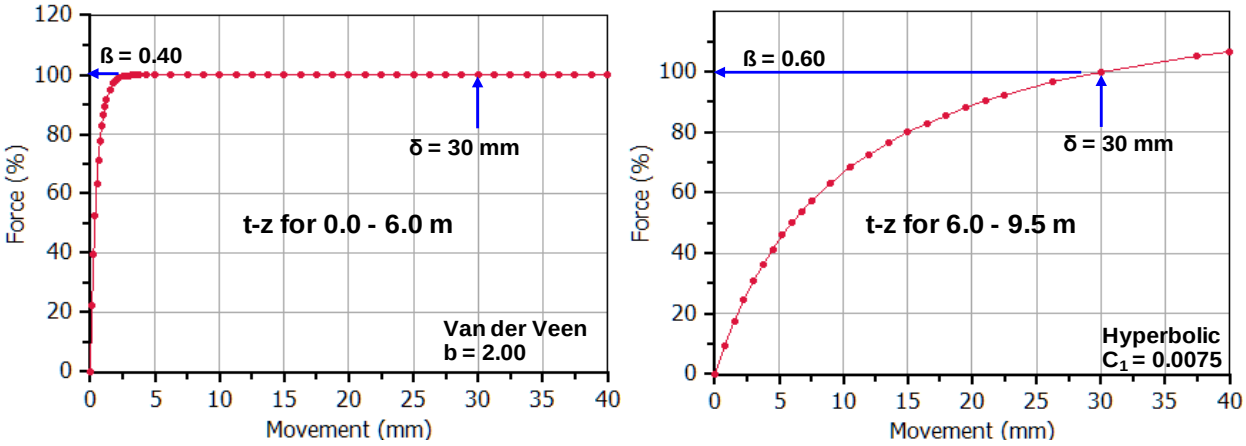

Fig. 6. Pile A3 t-z functions for the fit to the pile head load-movement curve.

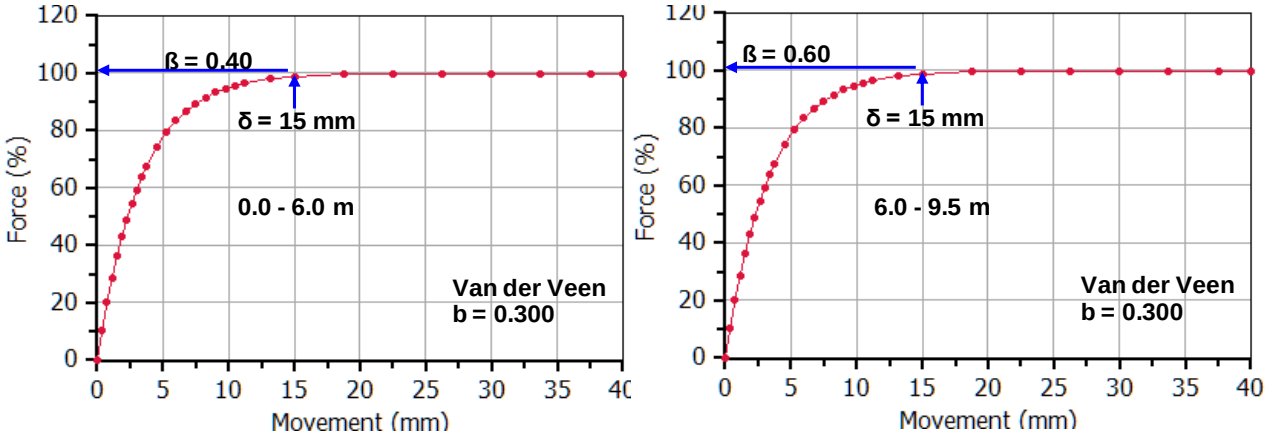

Fig. 7. Pile D2 t-z functions for the fit to the pile head load-movement curve.

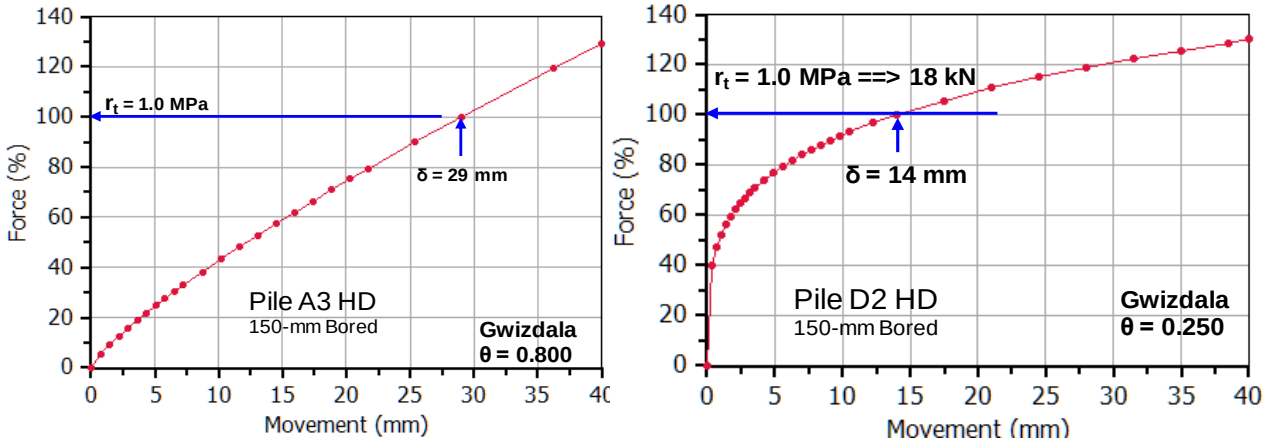

Fig. 8. Pile A3 and Pile D2 q-z functions for the fit to the pile head load-movement curve.

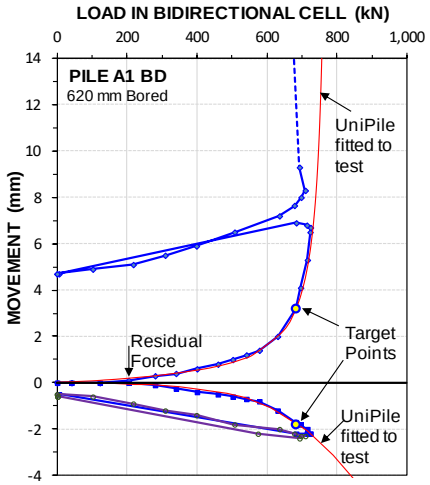

Fig. 9A. Pile A1 load-movement curves.

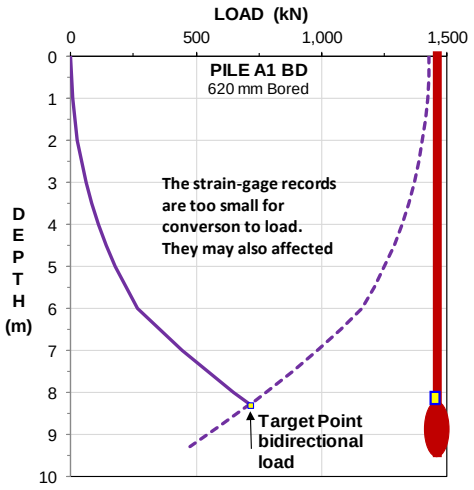

Fig. 9B. Pile A1 load distribution.

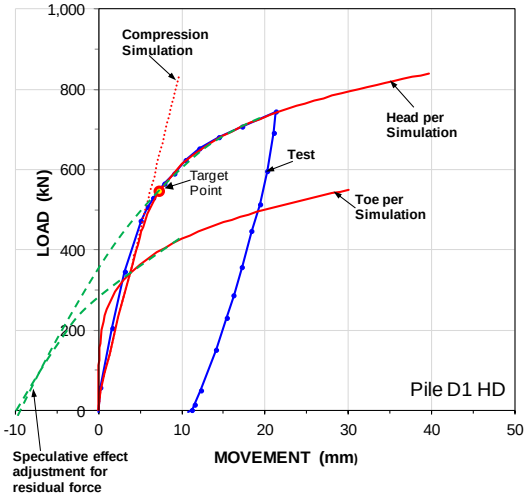

Fig. 10A. Pile D1 load-movement curves.

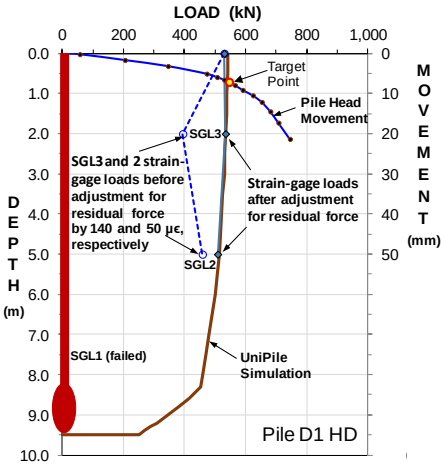

Fig. 10B. Pile D1 load distribution.

Micro piles, Piles D, with and without EB

For the micro piles, Piles D1 and D2, the beta-coefficients above the EB level (8.3 m) were the same as used for Pile D2 (and Piles A3 and A1). Below this depth, i.e., along the EB, the Pile D1 simulation fit showed ß = 1.50, i.e., more than twice that for Pile D2 along the same depth. The fitted unit toe resistance for Pile D1 was 2.0 MPa at 1 mm movement (corresponding to 3.8 MPa at 14 mm) as opposed to 1.0 MPa for Pile D2 at 14 mm movement. The t-z and q-z function produced in the fitting show that the EB had not just provided a larger resistance, it had also stiffened up the response of the pile.

The load-movement curves and load distributions for the two micro-piles bored with slurry, gravity-grouted (Piles-D) are compared in Figures 12A and 12B. The pile-head load-movement curves show that equipping the micro pile with the EB increased the total pile resistance about four times. No change in shaft resistance occurred above 8.3 m depth, while the resistance below 8.3 m depth, the EB zone, increased from 50 kN to 450 kN. Below 8.3 m depth, the unit shaft resistance along the EB and the unit toe resistance was more than about twice that of the pile with no EB. If the acceptable limit would be 5 to 10 mm movement (settlement) for an applied load, the EB-equipped micro pile would support an about three times higher load than the pile without an EB.

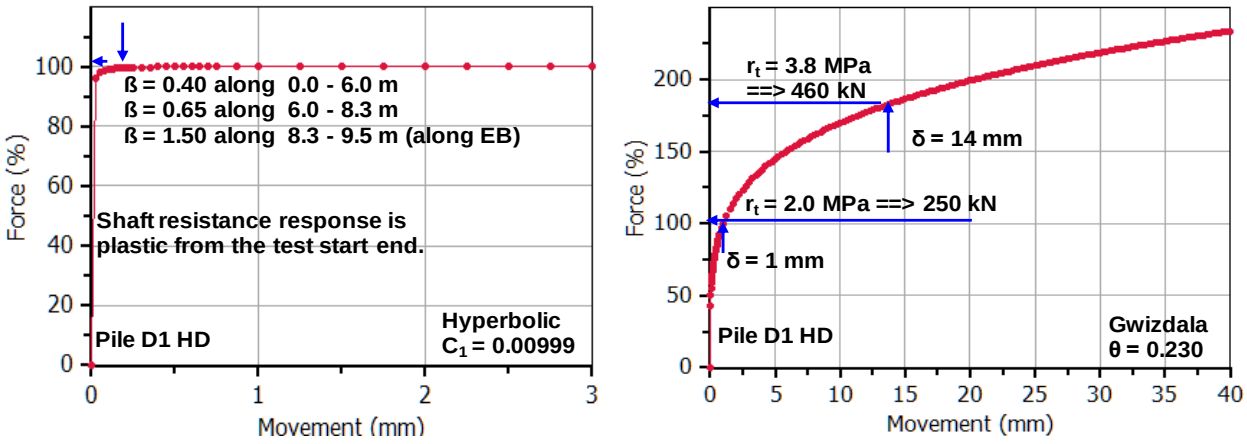

Fig. 11. Pile D1 t-z and q-z functions for the fit of the EB response.

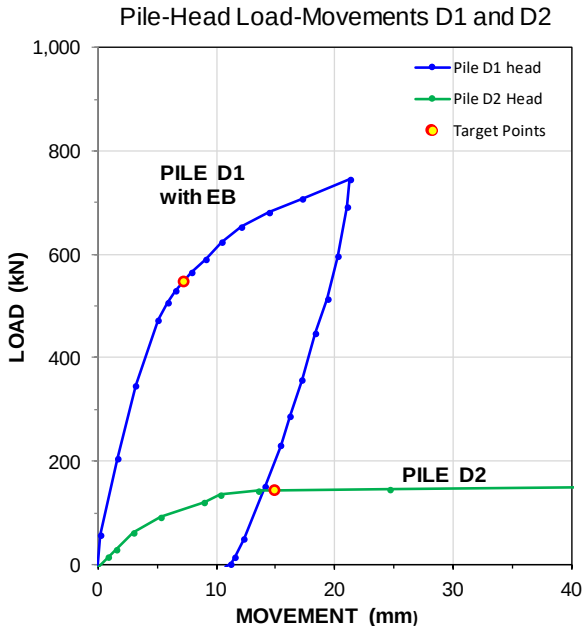

Fig. 12A. Piles D1 and D2 load-movement curves.

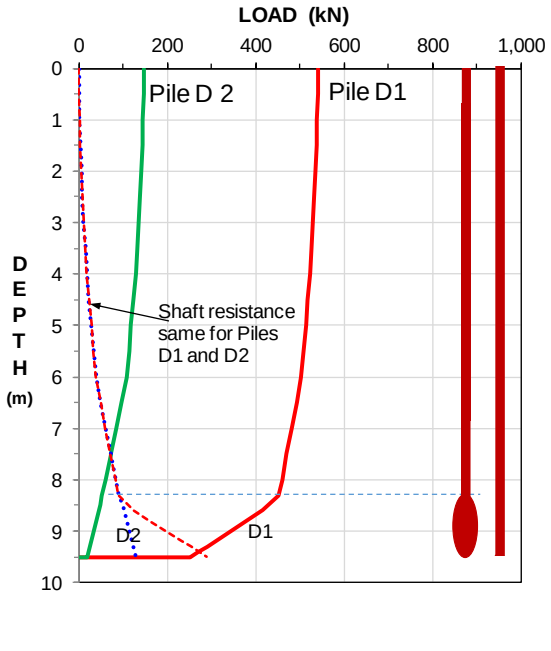

Fig. 12B. Piles D1 and D2 load distribution.

Bored piles, Piles A, with and without EB

For the 600-mm diameter bored piles, Piles A1 and A3, Figure 13A shows the Pile A1 actual downward test and the simulated downward test for Pile A3 calculated using UniPile from the conditions for the simulation by the head-down test. Similarly, Figure 13B show the Equivalent head-down test calculated from the simulation of the bidirectional test and the actual head-down test on Pile A3. Again, the comparison shows that the response of the EB-equipped pile was considerably stiffer than that of the unaugmented pile. As for Piles D, if the acceptable limit would be 5 to 10 mm movement (settlement) for an applied load, the EB-equipped Pile A1 pile would support an about three times higher load than Pile A3, the pile without an EB. To have about equal response, Pile A3 would have to be lengthened by about 6 m.

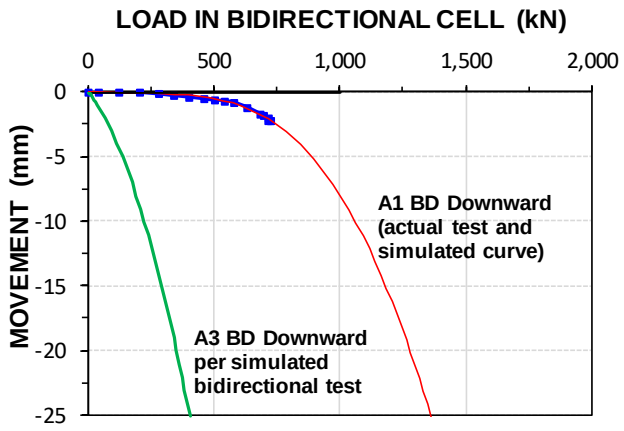

Fig. 13A. Piles A1 and A3 downward curves for a BD at 8.3 m depth.

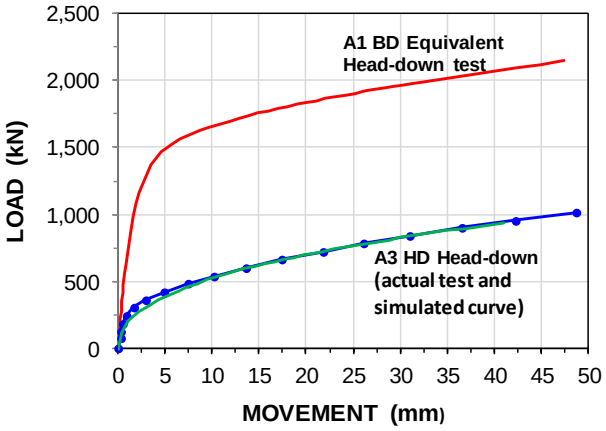

Fig. 13B. Piles A1 and A3 pile-head load-movements.

CFA piles, Piles B1 and B2, with and without EB

The 450-mm diameter CFA piles, Piles B1 and B2 were, 9.5 m long, pressure-grouted CFA piles with a nominally 0.159 m^2 cross section area. Pile B1 was equipped with an EB at 8.3 m depth, while Pile B2 was without an EB. Pile B1 was tested using a bidirectional cell placed immediately above the EB. Unfortunately, the telltale measuring the downward movement of the EB (the EB was the base of the bidirectional test) of Pile B1 test failed. That is, the test records only included the upward movements and the BD loads.

Piles B test records were analyzed similarly to the procedure used for the bored piles, Piles D and A, and showed that the unit shaft resistance along the CFA-constructed piles was stiffer than for the bored piles. In order to save space, the factual load-movement, load-distribution, and simulation results are not presented here. The can be examined at: http://www.cfpbolivia.com/web/page.aspx?refid=157. Figure14A compares the bidirectional downward curve of Pile B1 (movement measurement failed) to the similar curve simulated from the results of the head-down test on Pile B2calculated using UniPile. Similarly, Figure 14B shows the actual and simulated load-movement curves of the head-down test on Pile B2 and the equivalent head-down curve calculated from the simulation of the bidirectional test. Again, the comparison shows that the response of the EB-equipped pile, Pile B1, was considerably stiffer than that of the unaugmented pile, Pile B2. If the acceptable limit would be 5 to 10 mm movement (settlement) for an applied load, the EB-equipped pile would support about a twice higher load than the pile without an EB. To have about equal response, Pile B2 would have to be lengthened by about 3 m.

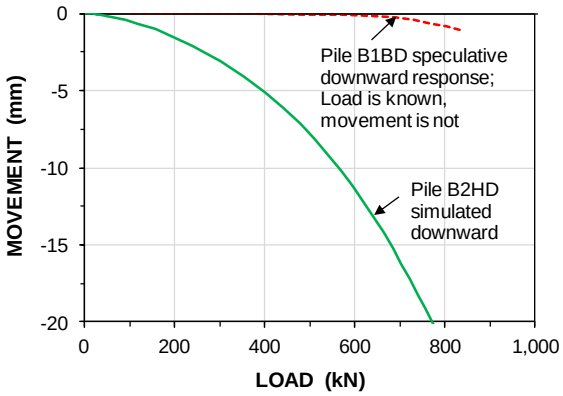

Fig. 14A. Piles B1 and B2 downward curves for a BD at 8.3 m depth.

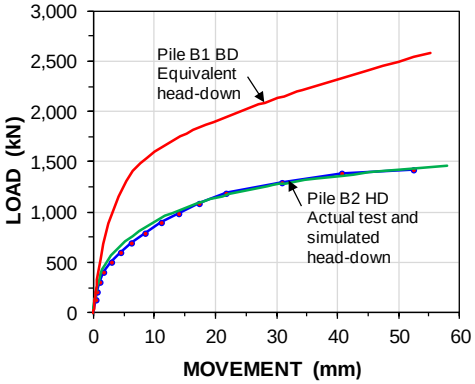

Fig. 14B. Piles B1 and B2 pile-head load-movements.

FDP piles, Piles C1 and C2, with and without EB

Piles C1 and C2 were 450-mm diameter, 9.5 m long, pressure-grouted, full-displacement (FDP) piles with a nominally 0.1590 m^2 cross section area. Pile C1 was equipped with an EB at 8.3 m depth, while Pile C2 was without an EB. Pile C1 was tested using a bidirectional cell placed immediately above the EB. Unfortunately, the records of the BD tests were lost. A head-down reloading test was carried out after first closing the 12-mm opening in the BD jack produced in the BD test. Again, in order to save space, the factual load-movement, load-distribution, and simulation results are not presented here. The results are available at: http://www.cfpbolivia.com/web/page.aspx?refid=157.

The analysis of Piles C test records showed that the unit shaft resistance was stiffer than for the bored piles. Figure 15 shows the load-movement curve of the head-down test on Pile C2 and the equivalent head-down curve calculated from the simulation of the bidirectional test. As was the case for Piles B, the comparison shows that the response of the EB-equipped Pile C1 was considerably stiffer than that of the unaugmented pile, Pile C2. If the acceptable limit would be 5 to 10 movement (settlement) for an applied load, the EB-equipped CFA-pile would support about an about 30 % higher load than the unaugmented pile. To have about equal response, Pile C2 would have to be lengthened by about 3 m. It is interesting to note that the response of the FDP pile was considerably stiffer than that of the CFA pile with or without the EB.

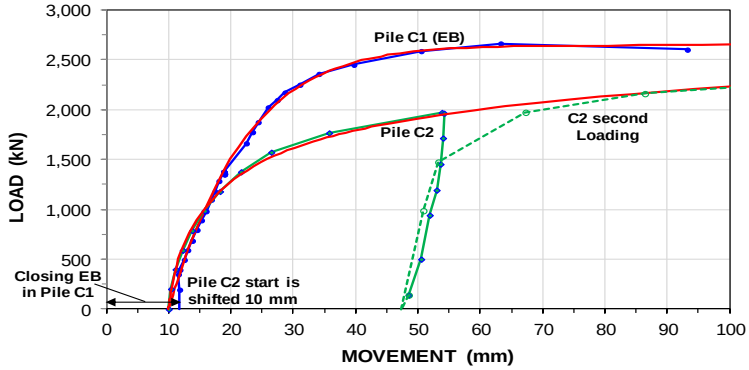

Fig. 15. Piles C1 and C2 pile-head load-movement curves.

CONCLUSIONS

For all four piles types, equipping the pile toe with the EB with post-installation grouting considerably increased the pile stiffness response to applied load. The improvement was largest for the micro-pile and the bored pile and smaller, but still significant, for the CFA and the FDP piles, as their construction methods improve the pile shaft resistance making the relative improvement of the toe less pronounced. Expansion of the EB is in a sense a loading test of the pile toe, assuring stiff pile response, enhanced capacity, and substantiation of the pile response, which also results in fewer piles and shorter construction time. The expansion of the EB resulted in imposing axial residual force in the piles further enhancing the pile stiffness. At site conditions similar to those at the subject site, the EB augment results in significant cost savings and enhanced quality control.

References

Fellenius, B.H., 2016. An Excel template cribsheet for use with UniPile and UniSettle. www.Fellenius.net.

Goudreault, P.A. and Fellenius, B.H., 2014. UniPile Version 5, User and Examples Manual. UniSoft Geotechnical Solutions Ltd. [www.UniSoftGS.com]. 120 p.

Terceros, M.H. and Massarsch, K.M, 2014. The use of the expander body with cast in-situ piles in sandy soils. Proceedings of the DFI-EFFC International Conference on Piling and Deep Foundations, Stockholm, May 21-23, pp. 347-358.